Methyl Motional Parameters in Crystalline L-Alanine: Molecular Dynamics Simulation and NMR

David C. Chatfield* and Sergio E. Wong

Chemistry Department, Florida International University, Miami, Florida 33199

Received: May 17, 2000; In Final Form: August 4, 2000

The correlation time for side-chain methyl reorientation in crystalline L-[β-$^2H_3$]alanine is calculated from molecular dynamics (MD) simulations and compared with NMR measurements. Correlation times for methyl reorientation may be a sensitive measure of packing in proteins, and characterizing the motions of side-chains is of interest for protein folding. Converged correlation functions were obtained by averaging over all side-chain methyls in the primary cell of MD simulations with periodic boundary conditions. When corrected for neglect of quantum mechanical tunneling, the correlation times from simulation are in excellent agreement with those from NMR, but this difference may not be significant. A torsional parameter in the CHARMM22 force field was reduced on the basis of ab initio calculations for use in the simulations, and the agreement between MD and NMR correlation times confirm that this was correct.

Introduction

The internal motions of proteins may be important for many processes in molecular biology, including protein folding and ligand binding. Motional parameters (order parameters and correlation times) for a number of proteins and peptides have been measured with NMR.[1−12] However, interpretation of NMR motional parameters requires a model for the motions that NMR cannot provide. Molecular dynamics (MD) simulation may provide a model for interpreting motional parameters. By now a considerable body of literature exists relating protein backbone order parameters derived from MD simulation to those obtained from NMR.[3,8,12−18] Trends with respect to secondary structure are in general reproduced. MD simulations have been used, for example, to evaluate motional models of backbone NH and $C_\alpha H$ bond vectors[8,16] and to relate order parameters to conformational entropy.[19−22]

The dynamics of amino acid side chains has not been studied as thoroughly as that of protein backbones. NMR measurements of some side-chain motional parameters have been reported,[5,7,9,10,23−25] but agreement with the few MD studies of side-chain motions is not nearly as good as that for backbones.[12,26] For example, we recently reported correlation times for alanine methyl reorientation from an MD simulation of staphylococcal nuclease. For half of the methyls, the correlation times were in qualitative agreement with values measured by NMR, but for the other methyls, the values from simulation were larger by an order of magnitude or more. Possible causes include the different time scales of NMR and MD (the NMR data represent the conformations sampled during a much longer time, and over a larger ensemble of molecules, than the 18 ns of MD simulation) and the limitations of the empirical force field.[26] Partly because of such difficulties, related systems of lower complexity, that is, small peptides, have been studied with NMR and MD. A salient example is the extensive work on the cyclic decapeptide antamanide.[27−32] We have chosen an even simpler system to elucide discrepancies such as those we encountered with SNase.

The work reported here focuses on methyl side chains of crystalline, zwitterionic L-[β-$^2H_3$]alanine. Hereafter, reference to alanine will mean the zwitterion form of L-alanine. Both the MD simulations, performed with periodic boundary conditions, and the ^2H NMR data, obtained from the powder pattern,[33,34] pertain to the crystalline state. The alanine methyls were deuterated in both the NMR experiments and the MD simulation. It is expected that focusing on the crystalline state will minimize the problem of adequately sampling conformational space on the MD time scale. For this reason, and because the time scale for methyl reorientation is in general smaller than that for longer side chains and thus more accessible to simulation, time scale differences are not expected to greatly influence the comparison between MD- and NMR-derived motional parameters. The goal is to assess the degree of agreement between MD and NMR for use in understanding larger systems and as a first step toward studying longer side chains. The dynamics of methyl groups in many polycrystalline amino acids, in particular alanine, has been measured with ^1H NMR[35−37] and ^2H NMR.[33,34,38,39]

The analysis reported below is based on MD simulations of crystalline alanine using periodic boundary conditions, beginning with an X-ray diffraction crystal structure.[40] Crystalline alanine has a particularly tightly packed structure that results in long correlation times for methyl reorientation.[33,34] Consequently, a relatively high temperature is needed to sufficiently sample the motion in a reasonably short simulation. Correlation times are obtained from autocorrelation functions for methyl reorientation. The crystal's symmetry enables us to obtain quite precise motional parameters from the correlation functions by averaging over equivalent methyls. The correlation times obtained from simulation are in excellent agreement with those measured with NMR after correcting for simulation's neglect of tunneling and NMR's use of a three-site jump model for the motion. The differences are probably not significant when uncertainties in experiment, simulation, and the ab initio methyl rotational barrier are considered.

* To whom correspondence should be addressed. E-mail: chatfiel@fiu.edu. Fax: (305) 348-3772.

10.1021/jp0018089 CCC: $19.00
Published on Web 11/05/2000

TABLE 1: Crystal Structures Used in Simulations[a,b]

N^c	space group	Z^c	*a*	*b*	*c*
1	$P2_12_12_1$	4	6.125	12.324	5.783
4	*P*1	4	6.125	12.324	5.783
32	*P*1	32	12.050	24.648	11.566

[a] All of the structures correspond to the same crystal type, but they differ in the space groups and lattice constants used to construct the crystal. [b] Lattice constants *a*, *b*, and *c* are in Å. [c] *N* is the number of primary (independent) molecules in the simulation. *Z* is the number of molecules in the unit cell.

Methods

Crystal Simulations. Simulations of crystalline L-[β-$^2H_3$]-alanine were performed with the program CHARMM.[41] Initial coordinates were taken from an X-ray diffraction crystal structure.[40] The structure is orthorhombic, belongs to the space group $P2_12_12_1$, and has four molecules per unit cell. The unit cell parameters are $a = 6.125$ Å, $b = 12.324$ Å, and $c = 5.783$ Å. The crystal was simulated with periodic boundary conditions. In such a simulation the crystal is divided into primary and image atoms, and only the former move independently. We performed several simulations to determine the dependence of simulated properties on the choice of primary atoms.

In the first simulation, the primary atoms corresponded to the crystallographic asymmetric unit, and the images were constructed from it using the symmetry operations of the $P2_12_12_1$ space group and the crystallographic lattice constants. In the second simulation, all four molecules in the crystallographic unit cell were primary. Their initial coordinates were constructed from the X-ray coordinates of the single molecule in the asymmetric unit and the symmetry operations of the $P2_12_12_1$ space group. The images were constructed from these atoms using the symmetry operations of the *P*1 space group and the crystallographic lattice constants. In the third simulation, the dimensions of the unit cell were doubled, and 32 molecules were primary. Initial coordinates were constructed by translating copies of primary atoms in the second simulation by distances equal to the crystallographic lattice constants along the respective lattice axes. The images were constructed using the symmetry operations of the *P*1 space group and lattice constants double those of the crystallographic unit cell.

The crystal structures used in simulations are summarized in Table 1. In this table, *N* is the number of primary molecules, the images are constructed with the symmetry operations of the space group and the lattice constants listed, and *Z* is the number of molecules in the corresponding unit cell. Note that only for $N = 1$ are the space group, *Z*, and lattice constants the same as those for the X-ray crystal structure.

MD simulations employed the all-atom CHARMM22 parameter set[42] with a modification to the methyl torsional parameter described below, and with the mass of alanine methyl hydrogens increased to represent deuterium. Electrostatics were treated with the particle-mesh Ewald method,[43,44] using a fifth-degree B-spline interpolation and 10^{-5} tolerance set for the direct space sum cutoff. van der Waals interactions were treated with the shift method using a 10-Å cutoff.[45] NVE simulations were performed with the leapfrog Verlet integrator using a 1-fs time step. Unless otherwise specified, the temperature was 362 K, the highest temperature for which NMR correlation times are available.[33]

The simulations were initiated at 100 K, heated to 362 K over 15 ps, and equilibrated at 362 K for 35 ps. The $N = 4$ and $N = 32$ simulations were then continued for 25 and 3.125 ns, respectively, and these portions of the trajectories were analyzed.

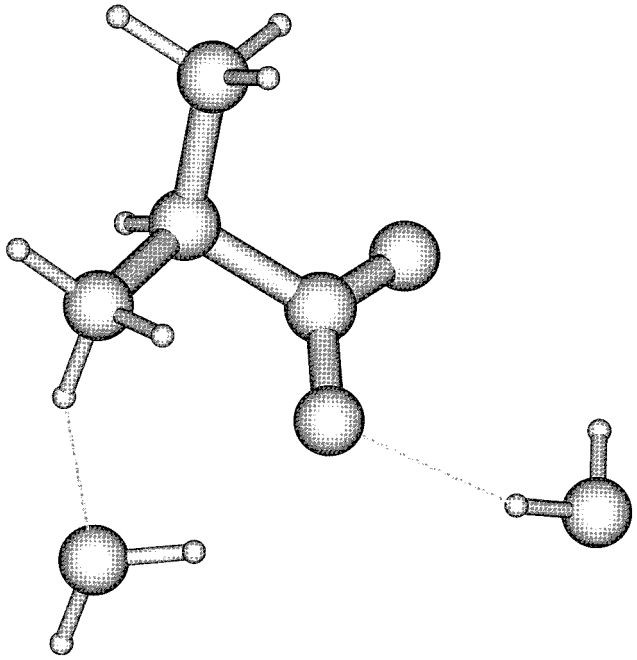

Figure 1. HF/6-31G optimized conformation of zwitterionic L-alanine hydrated with two waters.

The product of *N* and the simulation length is 100 ns for both simulations. Thus, the average correlation function for methyl rotation, $C(t)$ (see definition below), is expected to be equally well converged in the two cases, although the individual correlation functions, $C_i(t)$, will be better converged for $N = 4$ than for $N = 32$.

Methyl Torsional Parameters. Before MD simulations were performed, a torsional term in the CHARMM22 parameter set was adjusted to reproduce ab initio values for the methyl rotational barrier. Simulations probing methyl reorientation in proteins have also had to adjust CHARMM force fields to achieve reasonable barriers to rotation.[26] We calculated ab initio methyl adiabatic rotational barriers for an isolated alanine zwitterion with Gaussian92.[46] Two waters were included to stabilize the zwitterion, as otherwise a proton was transferred from the NH_3^+ to the CO_2^- during optimization. The barriers obtained at the HF/6-31G, HF/6-31++G(D,P), and MP2//HF/6-31G levels, using constrained optimization, were 3.76, 3.73, and 3.59 kcal/mol, respectively. The fully relaxed system is shown in Figure 1.

Restrained optimization with CHARMM using the CHARMM22 parameter set produced an adiabatic barrier of 4.74 kcal/mol, about 1.0 kcal/mol too high. Dihedral, electrostatic, and van der Waals terms all contributed to the barrier. To correct for this discrepancy, the force constant k_ϕ for dihedral angle terms contributing to the barrier was reduced from 0.200 to 0.145 kcal/mol. This choice was made as follows. In the CHARMM22 parameter set, each set of four atoms having bonded connectivity contributes one dihedral energy term to the total energy. For methyl rotation nine such terms contribute to the barrier. The atom types of alanine α- and β-carbons are CT1 and CT3, respectively, and the force constant for all dihedral terms of type X-CT1-CT3-X, where X is any atom, is 0.200 kcal/mol. The energy term E_ϕ for dihedral angle ϕ has the form $E_\phi = k_\phi(1 + \cos 3\phi)$, so each term for methyl rotation contributes approximately $2k_\phi = 0.400$ kcal/mol to the adiabatic barrier. Thus, reducing k_ϕ to 0.145 kcal/mol is expected to reduce the barrier by $\approx(9 \times 2 \times 0.055) = 0.990$ kcal/mol. In fact, the adiabatic barrier calculated using the modified k_ϕ is

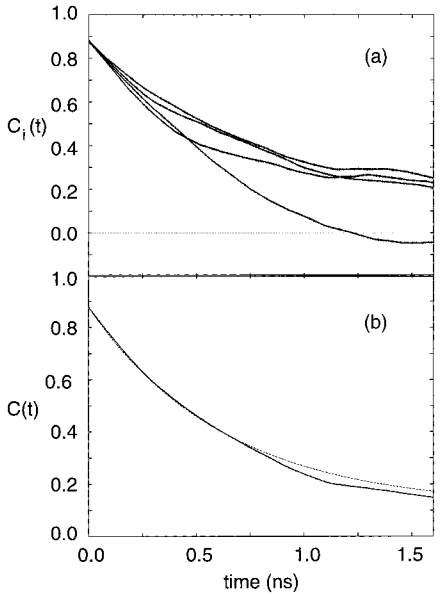

Figure 2. (a) Individual correlation functions from the $N = 4$ MD simulation of crystalline alanine. (b) Average of the individual correlation functions in (a) (solid curve) and the fit obtained with eq 5 (dashed curve).

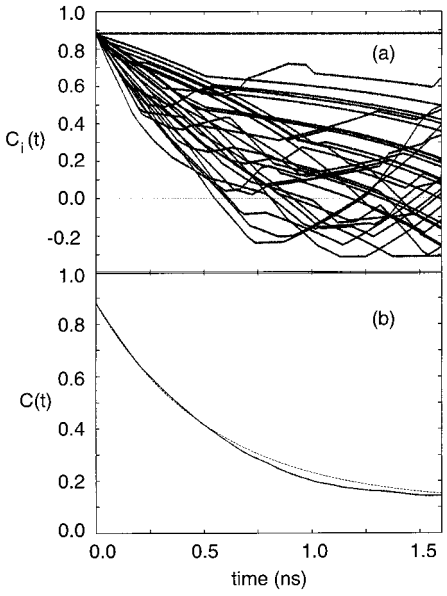

Figure 3. Like Figure 2, but for $N = 32$.

3.75 kcal/mol, in agreement with the ab initio values. The modified parameter was used in all calculations described below unless otherwise specified.

Correlation Times τ_e. Correlation times τ_e were computed from correlation functions $C_i(t)$ calculated from the MD trajectories. The correlation function for reorientation of a bond vector $\hat{\mu}_i$ of unit length is

$$C_i(t) = \langle P_2(\hat{\mu}_i(0)\cdot\hat{\mu}_i(t))\rangle \tag{1}$$

where $P_2 = {}^3/_2x^2 - {}^1/_2$ is a second Legendre polynomial. A simulation of finite length yields the approximation

$$C_i(t_M) = \frac{1}{N_{\text{pts}} - M}\sum_{j=1}^{N_{\text{pts}} - M}\langle P_2(\hat{\mu}_i(t_j)\cdot\hat{\mu}_i(t_{j+M}))\rangle \tag{2}$$

where the MD trajectory consists of conformations at N_{pts} equally spaced points in time. In practice, the approximation will be reliable only when the time scales for the underlying dynamical processes are much less than the total simulation time. This can present a significant computational challenge for large systems. For a crystal, though, we can take advantage of the periodicity and average over all equivalent bond vectors. Thus, for a simulation with N primary alanines (Table 1), we average the correlation functions for reorientation of all the $C_\beta H$ bond vectors,

$$C(t) = \frac{1}{N}\sum_{i=1}^{N} C_i(t) \tag{3}$$

where $C_i(t)$ are the individual correlation functions and $C(t)$ is the average. Examples of averaged and unaveraged correlation functions for $N = 4$ and $N = 32$ are shown in Figures 2 and 3. (Only one of the three $C_\beta H$ bond vectors, arbitrarily chosen as CB−HB1 in CHARMM notation, was included for each methyl.)

If the motion of a bond vector represents a process or group of processes occurring on a single time scale, it is appropriate to calculate a generalized order parameter, S, and a correlation time, τ_e, according to the Lipari and Szabo definition:[47]

$$C(t) = S^2 + (1 - S^2)e^{-t/\tau_e} \tag{4}$$

For a methyl group with C_{3v} symmetry, S^2 has the value $[(3\cos^2\beta - 1)/2]^2$ where β is the $C_\alpha C_\beta H$ angle. For ideal tetrahedral geometry ($\beta = 109.5°$), S^2 equals ${}^1/_9$.

Very fast initial decay of $C(t)$ to 0.878, which corresponds to fast libration of the $C_\beta H$ and $C_\alpha C_\beta$ bonds, is observed in Figures 2 and 3. When this initial decay is taken into account, assuming that the librational motions are very fast compared to rotation about the methyl symmetry axis, and for a methyl with ideal tetrahedral geometry, eq 4 is replaced with

$$C(t) = \frac{1}{9} + \left[C(0+) - \frac{1}{9}\right]e^{-t/\tau_e} \tag{5}$$

where $C(0+)$ is the value of $C(t)$ immediately after the initial, fast decay. Correlation times for single-exponential fits were calculated by nonlinear least-squares fitting of $C(t)$ by eq 5, using the Levenberg−Marquardt method.[48]

Results

Rotational Barriers. To determine how large a primary cell would probably be needed to accurately represent the dynamics in an MD simulation, methyl rotational barriers were calculated for crystal models with primary cells containing 1, 4, and 32 alanines, and also, for comparison, for a single, isolated alanine. Both rigid and adiabatic barriers were calculated and are given in Table 2, along with the barrier from the potential of mean force (pmf) calculated from the MD simulations, as described below. The rotational barrier is of course smallest for the isolated molecule. The barrier for the crystal is unrealistically high when $N = 1$ because the model is too inflexible. However, the barrier is quite well converged by $N = 4$. The rigid barrier is nearly constant as N is increased from 4 to 32, and the adiabatic barrier, although decreasing by a small amount (0.07 kcal/mol), also appears well converged. Still, one could imagine a priori that the size of the primary cell might influence correlation times via dynamical effects as well as via the adiabatic barrier. Therefore, simulations were performed for both $N = 4$ and $N = 32$ for comparison.

TABLE 2: Methyl Rotational Barriers (kcal/mol) for Alanine Zwitterion

N	rigid[a]	adiabatic[b]	pmf	*N*	rigid[a]	adiabatic[b]	pmf
c	4.16	3.75	3.7	4	6.36	5.62	6.1
1	16.06	7.28		32	6.35	5.55	6.0

[a] The rigid rotational barrier was evaluated for all four independent methyls for $N = 4$ and found to be identical. [b] The variation of the adiabatic rotational barrier with the position of the methyl within the primary cell was investigated for a model with $N = 108$. Methyls on the interior and exterior of the primary cell both had adiabatic rotational barriers of 5.54 kcal/mol. [c] In this row, the rigid and adiabatic barriers were calculated for an isolated (gas phase) alanine zwitterion, and the pmf is from a Langevin dynamics simulation, i.e., with stochastic and dissipative forces to simulate a solvent environment.

TABLE 3: Correlation Times (ps) from Fit by Eq 5[a]

N	τ_e	τ_e^n	$^2/_3\bar{t}_w$	*N*	τ_e	τ_e^n	$^2/_3\bar{t}_w$
4	630 ± 70	650 ± 70	740 ± 70	32	540 ± 60	550 ± 60	620 ± 50

[a] A value of 0.878 was used for $C(0+)$ in eq 5.

TABLE 4: Contributions (kcal/mol) to the Difference between the Crystal- and Gas-Phase Methyl Rotational Barriers ($\Delta\Delta E$)[a]

	$\Delta\Delta E$	
terms	rigid[b]	adiabatic[c]
bonded[d]	−0.43	−0.38
van der Waals[e]	2.77	1.60
electrostatic[f]	0.25	0.65
total	2.59	1.87

[a] $\Delta\Delta E$ is defined in eq 6. [b] For rigid rotation. [c] For adiabatic rotation. [d] Includes bond, angle, dihedral, improper, and Urey contributions. [e] Includes van der Waals and image van der Waals contributions. [f] Includes electrostatic and image electrostatic contributions.

We determined the dominant contributions to the difference between the crystal- and gas-phase methyl rotational barriers, $\Delta\Delta E$. Analysis of the pmfs would be most pertinent, but analysis of the rigid and adiabatic rotational barriers is more straightforward, and we expect it to yield similar information. Thus, we define $\Delta\Delta E$ by

$$\Delta\Delta E = (E_{max} - E_{min})_{crystal} - (E_{max} - E_{min})_{gas} \qquad (6)$$

where E_{max} and E_{min} are the maximum and minimum energies during rotation. The contributions to $\Delta\Delta E$ from bonded, van der Waals, and electrostatic terms are given in Table 4 (the $N = 4$ crystal model was used). The bonded terms make a negative contribution, primarily because van der Waals interactions shift the barrier maximum away from 0° in the crystal, and thus the dihedral terms contribute less to the barrier in the crystal than in the gas phase. The van der Waals terms make the largest contribution to $\Delta\Delta E$. The value of $\Delta\Delta E$ is 0.74 kcal/mol smaller for adiabatic than for rigid rotation, primarily due to a 1.17 kcal/mol smaller van der Waals contribution that is only partially offset is offset by a larger electrostatic contribution. van der Waals interactions with just four atoms in neighboring molecules (C and O in one and C_β in each of two others) account for 68% of the adiabatic and 70% of the rigid $\Delta\Delta E$. Many electrostatic interations make contributions of large magnitude (0.5−2 kcal/mol), but they mostly cancel out. The individual electrostatic contributions differ significantly between the rigid and adiabatic cases. Thus, we propose the conceptual picture of a few van der Waals interactions that account for most of $\Delta\Delta E$, together with a "bath" of electrostatic interactions that contribute a smaller amount and, depending on the circumstances, may be important for relaxation.

Correlation Functions. Correlation functions for $C_\beta H$ bond reorientation are shown in Figure 2 for $N = 4$ and in Figure 3 for $N = 32$. In both figures, the upper panel shows the individual $C_i(t)$, and the lower panel shows the average, $C(t)$. The improvement upon averaging is particularly striking for $N = 32$. Clearly, 3.125 ns is too short to converge the individual $C_i(t)$ for $N = 32$, but $C(t)$ exhibits a smooth decay up to 1.6 ns. The minimum value of just under −0.3 that several of the $C_i(t)$ exhibit is a consequence of only one or a few torsional transitions being made, as $P_2(\cos 109.5°)$ is $-^1/_3$.

Correlation times τ_e obtained by fitting $C(t)$ with eq 5 are given in Table 3. Uncertainties were estimated as $(2\tau_e/NT_{sim})^{1/2}$, where T_{sim} is the simulation time.[49] Although not apparent in Figures 2 and 3 because of their scale, $C(t)$ oscillates at very short times. The amplitude of the oscillations is damped from about 0.08 to a negligible amount by 3 ps. Linearly extrapolating $C(t)$ between 3 and 5 ps back to $t = 0$ yields a value of 0.878 for $C(0+)$, and this value was used in the fits summarized in Table 3. The oscillatory behavior of $C(t)$ at short time is due to small-angle vibrations and has been discussed elsewhere.[15] For a simulation of finite length, the degree of convergence of $C(t)$ decays as t increases. In view of this, the parameters in Table 3 were obtained by fitting only the initial portion of $C(t)$ (in particular, up to $t = 820$ ps for $N = 4$ and $t = 680$ ps for $N = 32$) and constraining S^2 to be $^1/_9$. The fitted functions are shown as dashed curves in Figures 2b and 3b, and the fits appear to be good.

To test whether the averaging procedure introduces bias, the $N = 4$ trajectory was split into eight different sections to simulate the analysis of the $N = 32$ data. Individual correlation functions $C_i(t)$ were calculated for each section and then averaged. When plotted, the resulting correlation function $C(t)$ was indistinguishable up to 700 ps from the correlation function obtained without splitting. It was concluded that averaging over different numbers of primary methyls does not introduce bias. We emphasize that averaging is appropriate because the methyls in the primary cell are equivalent, and because the NMR relaxation times represent averages over all methyls in the crystal.

Number Correlation Function. Also given in Table 3 are two quantities obtained by imposing a three-site jump model on the methyl dynamics: the correlation time τ_e^n obtained by fitting the number correlation function, $C^n(t)$, and $^2/_3\bar{t}_w$, where $\bar{t}_w$ is the average waiting time between jumps. The number correlation function, like $C(t)$, is calculated with eqs 1 and 3. However, in this case $\hat{\mu}_i$ in eq 1 is only allowed the orientations $\hat{\mu}^1$, $\hat{\mu}^2$, and $\hat{\mu}^3$ of a methyl with perfect tetrahedral geometry hopping between minima at $\phi = 60°$, 180°, and 300°. The orientations are obtained from the MD trajectory by setting $\hat{\mu}_i = \hat{\mu}^1$ if $0° \le \phi < 120°$, $\hat{\mu}_i = \hat{\mu}^2$ if $120° \le \phi < 240°$, and $\hat{\mu}_i = \hat{\mu}^3$ if $240° \le \phi < 360°$, where ϕ is the $N-C_\alpha-C_\beta-H_{\beta1}$ dihedral angle and where $H_{\beta1}$ is an arbitrary but consistently chosen methyl hydrogen. The number correlation functions obtained from the $N = 4$ simulation are shown in Figure 4. This figure is nearly indistinguishable from Figure 2.

For a methyl executing three-site jumps, it can be shown that the correlation time is equal to two-thirds of the average waiting time between jumps. To calculate $\bar{t}_w$ from an MD trajectory, it is necessary to define a jump, that is, a rotational transition. It is important not to overcount the number of barrier crossings.[29,30,50] Thus, we define a methyl as being in state A, B, or C if ϕ maintains a value of 20°−70°, 110°−220°, or 260°−340°, respectively, for at least 5 ps. Then, $\bar{t}_w$ is the average time between transitions between these states. Statistics were also obtained using other values for the limits on duration and angle

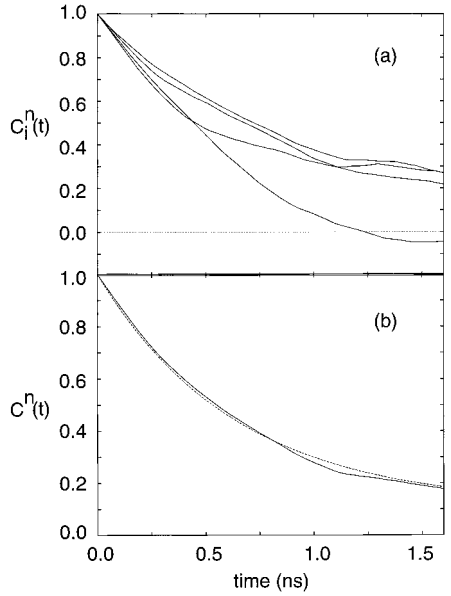

Figure 4. Like Figure 2, but for the number correlation functions.

range, and the values listed above were found to be reasonably robust. The reader is directed to ref 50 for a fuller discussion of counting statistics for barrier crossings. The uncertainties (standard errors) in $^2/_3\bar{t}_w$ in Table 3, obtained assuming a normal distribution of waiting times, are in good agreement with the uncertainties in τ_e. The uncertainties can also be obtained by regarding the methyl dynamics as a Poisson process[51] and considering the number of jumps. The confidence intervals for the number of jumps, assuming a Poisson distribution, can be found in standard tables.[52] These are in good agreement with the uncertainties in $^2/_3\bar{t}_w$ given in Table 3, as expected since Poisson and normal distributions yield similar uncertainties when the number of events is large (here 87 jumps for $N = 4$ and 109 jumps for $N = 32$).[53] In any case, for both simulations τ_e and τ_e^n are very close, and although smaller than $^2/_3\bar{t}_w$, they are within the uncertainty. The agreement among these three quantities supports the accuracy of the fitted parameters and the appropriateness of the three-site jump model for interpreting the dynamics.

PMFs. PMFs were calculated from MD simulations using the relationship

$$W = -RT \ln p \tag{7}$$

where $W(\phi)$ is the pmf and $p(\phi)$ is the probability distribution for the $NC_\alpha C_\beta H$ torsional angle from the simulation. Some of the pmfs so obtained were somewhat jagged near the barrier top due to poorer sampling there, so the barrier height was estimated by fitting with the function

$$W(\phi) = E_0 + V\left[\frac{1 + \cos(3(\phi + a))}{2}\right]^b \tag{8}$$

where E_0 is an arbitrary zero of energy, V is the barrier height, a allows the barrier maximum to be shifted from 0° (by, for example, steric interactions with neighboring molecules), and b allows the contour to be narrow or wide. Sample pmfs and fits are shown in Figure 5. The barriers calculated from the pmf are shown in Table 2. The entry in the first row was obtained from a Langevin dynamics[54,55] (LD) simulation of a single alanine. LD models a solvent by stochastic and dissipative forces, propagating the dynamics of the solute according to the Langevin equation.[56] The pmf barrier was insensitive to variation

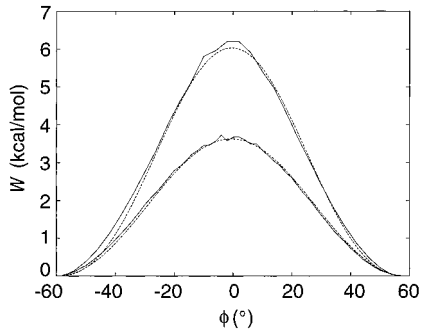

Figure 5. Potentials of mean force (W) from the $N = 4$ simulation of crystalline alanine (upper curves) and an LD simulation of a single alanine (lower curves). The solid curves are the pmf's from eq 7, and the dashed curves are fits by eq 8.

of the collision frequency, γ, in the range $0.1-100$ ps^{-1} and of the temperature in the range 298−700 K. The average barrier determined from the LD pmfs, 3.7 kcal/mol, is in agreement with the gas-phase adiabatic barrier, 3.75 kcal/mol. However, pmfs calculated from the crystal simulations yielded barriers intermediate between the rigid and adiabatic barriers. This suggests, interestingly, that in solution the molecule is able to distort its conformation during barrier passage; while in the crystal the requisite distortions, which may involve neighboring molecules, do not readily occur. Like the rigid and adiabatic barriers, the pmf barriers for $N = 4$ by $N = 32$ were nearly the same.

Sources of Error. Neglect of quantum mechanical tunneling will cause the correlation times calculated from the MD simulations to be overestimated. The error thus introduced was estimated by comparing, for a related one-dimensional problem, the rate constants calculated from transition state theory and from quantum mechanical tunnel splittings.[57,58] For rotation about a symmetric, sinusoidal 3-fold barrier of height V_0, the Schrödinger equation is

$$-\frac{\hbar^2}{2I}\frac{d^2\psi}{d\phi^2} + \left[-E + \frac{V_0}{2}(1 + \cos(3\phi))\right]\psi = 0 \tag{9}$$

where I is the moment of inertia and $\hbar$ is Planck's constant (h) divided by 2π. This equation can be written in the form of the Mathieu equation and solved analytically for the eigenvalues E, using software freely available.[59,60] The rate constant, k_{QM}, is obtained by Boltzmann averaging over the tunnel splittings,

$$k_{QM} = \frac{1}{\sum_{i=0}^{\infty} e^{-\bar{E}_i/RT}} \sum_{i=0}^{\infty} \upsilon_i e^{-\bar{E}_i/RT} \tag{10}$$

where

$$\upsilon_i = \frac{2\Delta E_i}{h} \tag{11}$$

and where $\bar{E}_i$ is the average of a pair of eigenvalues, ΔE_i is the difference between the pair of eigenvalues, and υ_i is a tunneling frequency.[57,58] Equation 10 contains a number of assumptions whose effect on the terms increases as the eigenvalues increase.[58] However, for the barrier and temperature studied here the rate constant is converged to within 5% by the fifth pair of eigenvalues above the barrier; the average energy of this pair of eigenvalues is only 37% greater than the barrier height.

Using a value of 6.0 kcal/mol for V_0 (close to the pmf barrier for crystalline alanine) in eq 9 with a temperature of 362 K and the moment of inertia of a deuterated methyl, and applying eqs 10 and 11, yields a k_{QM} of 2.74 GHz. Transition state theory, which of course neglects tunneling, yields a rate constant, $k_{TST} = (\omega/2\pi)e^{-V_0/RT}$, of 1.57 GHz, 43% smaller than k_{QM}. An alternative measure of the importance of tunneling is the contribution of sub-barrier eigenvalues to k_{QM}. This is 24% of k_{QM} for a 6.0 kcal/mol barrier. This measure of tunneling is somewhat arbitrary because it neglects the effect of nonclassical reflection above the barrier. However, for barriers between 5.3 and 6.8 kcal/mol, the contribution of sub-barrier tunneling varies nonmonotically between 16% and 37% of the total rate constant, depending on the difference between V_0 and the highest sub-barrier pair of eigenvalues. The various estimates of the error are of the same magnitude though not identical, and the least arbitrary is the one involving k_{TST} directly. For a three-site jump model, k and τ_e are related by $k = 1/3\tau_e$. Thus, we conclude that the value of k from the simulations of crystalline alanine is probably underestimated by about 43%, and likewise τ_e is overestimated by 43%, due to neglect of quantum mechanical tunneling.

Another source of error is the use of a three-site jump model to calculate correlation times from NMR data. This will be roughly estimated in the extreme narrowing limit. In this limit, the relationship between T_1 and τ_e can be expressed as[61]

$$\frac{1}{T_1} = \frac{4\omega_Q{}^2\tau_e}{27}[2 + f(1 + 3\cos^2(\theta))] \qquad (12)$$

where T_1 is the spin−lattice relaxation time, θ is the angle between the methyl symmetry axis and the external magnetic field, $\omega_Q = (3e^2qQ/(4\hbar))$, and e^2qQ is the quadrupole coupling constant. The parameter f varies between 1 for the three-site jump model and 0 for free diffusion. Calculating f requires solution of a Smoluchowski equation for one-dimensional diffusion in a 3-fold potential. This has been done for a 3 kcal/mol barrier, yielding a value of 0.76 for f.[61,62] Hence, using a three-site jump model in this case would cause τ_e to be underestimated by from 8% for $\theta = 90°$ to 16% for $\theta = 0°$. The parameter f could also be calculated for a 6 kcal/mol barrier, but we simply note that the error caused by applying a three-site jump model will be smaller for the higher barrier. Thus, for crystalline alanine we expect use of a three-site jump model to cause the values of τ_e from NMR to be underestimated by no more than about 10%.

Discussion

Correlation times of 280 and 310 ps for methyl reorientation have been determined from ^{2}H spin−lattice relaxation times of polycrystalline alanine at 362 K.[33] The two values represent analysis of the $\theta = 0°$ and 90° edges of the powder pattern, respectively. Thus, the experimental value for τ_e can reasonably be taken to be 295 ± 15 ps.[33] Adjusting this figure upward by 10% to roughly correct for the use of a three-site jump model yields a τ_e of 325 ± 15 ps.

The MD correlation times reported here might suggest a dependence on N, but the difference is less than the uncertainty, so we represent the simulated τ_e with the average value of 585 ± 90 ps. Adjusting the simulated τ_e downward 43% to correct for the neglect of tunneling yields 330 ± 50 ps. Thus, MD and experiment are in excellent agreement. We note that a reduction in the rotational barrier of just 0.17 kcal/mol (corresponding to the range of ab initio adiabatic barriers) would reduce the MD value by a factor of 0.79, assuming an Arrhenius relationship.

On the other hand, using the standard torsional parameters rather than the modified ones used here would increase the rotational barrier by 1.0 kcal/mol and τ_e by a factor of 4, clearly unrealistic. Thus, methyl correlation times in the solid state provide a useful experimental test for molecular mechanics force field parameters. The work reported here suggests that the CHARMM22 X-CT1-CT3-X torsional term is too large and should be reduced by 0.055 kcal/mol. One can, of course, correct τ_e post facto to represent a different barrier. However, a simulation run with a larger barrier will have poorer barrier crossing statistics and require correspondingly longer simulation times to achieve comparable uncertainties.

Figures 2 and 3 demonstrate clearly the advantage of averaging over equivalent bond vectors to converge correlation functions. This is especially useful when, as here, the accurate representation of the dynamics requires that several molecules, not just the crystallographic asymmetric unit, be included among the primary atoms.

At least three experimental measurements of the activation energy, E_a, for methyl rotation in crystalline L-alanine have been reported, two[33,34] from ^{2}H NMR and one[36] from ^{1}H NMR. All find E_a to be in the range 5.3−5.40 kcal/mol, based on the relationship $\tau_c = \tau_0 e^{-E_a/RT}$. Values of E_a could be obtained in an analogous manner from MD simulations at different temperatures, but this has not yet been done because of the cost. One can, however, compare the experimental E_a with the pmf barrier from simulation, 6.1 kcal/mol (the value from the $N = 32$ simulation). Even if this is reduced to correct for neglect of tunneling, it is larger than experiment. Possible causes can be postulated, but that remains a matter for further investigation. Carrying out long simulations at several temperatures might resolve these questions. That is beyond the scope of this project but would be worth pursuing, particularly for crystalline amino acids with smaller rotational barriers such as isoleucine and valine,[34,36] as the simulations could be shorter.

It has been suggested that correlation times for methyl reorientation may be a sensitive measure of packing in proteins.[26,33] This research is a first step toward quantifying the level of agreement between experiment and MD, and thus of MD's predictive capability. We have established that, for a small molecule such as alanine, a single crystallographic asymmetric unit may be too small a system for accurate simulation of the dynamics using MD with periodic boundary conditions. For crystalline alanine we have shown that when the primary system is of sufficient size and reasonable torsional parameters are used, MD correlation times are in excellent agreement with those measured with ^{2}H NMR. In general, other crystalline amino acids have a range of activation energies smaller than that of alanine, which has a particularly tight crystal packing.[40] If in future work MD can reproduce the experimental ordering of correlation times and activation energies for methyl rotation among other crystalline amino acids and peptides, the groundwork will be laid for extension to proteins.

Acknowledgment. We would like to thank Attila Szabo, Bernard Brooks, Richard Pastor, and Dennis Torchia for many useful discussions. This work was supported in part by the National Institutes of Health under Grant GM08205.

References and Notes

(1) Clore, G. M.; Szabo, A.; Bax, A.; Kay, L. E.; Driscoll, P. C.; Gronenborn, A. M. *J. Am. Chem. Soc.* **1990**, *112*, 4989−4991.

(2) Schneider, D. M.; Dellwo, M. J.; Wand, A. J. *Biochem.* **1992**, *31*, 3645−3652.
(3) Eriksson, M. A. L.; Berglund, H.; Härd, T.; Nilsson, L. *Proteins: Struct., Func., Genet.* **1993**, *17*, 375−390.
(4) Alexandrescu, A. T.; Shortle, D. *J. Mol. Biol.* **1994**, *242*, 527−546.
(5) Torchia, D. A.; Nicholson, L. K.; Cole, H. B. R.; Kay, L. E. In *Topics in Molecular and Structural Biology*; Clore, G. M., Gronenbaum, A. M., Eds.; MacMillan: London, 1993; pp 190−219.
(6) Farrow, N. A.; Zhang, O.; Forman-Kay, J. D.; Kay, L. E. *Biochem.* **1995**, *34*, 868−878.
(7) Buck, M.; Boyd, J.; Redfieold, C.; MacKenzie, D. A.; Jeenes, D. J.; Archer, D. B.; Dobson, C. M. *Biochemistry* **1995**, *34*, 4041−4055.
(8) Yamasaki, K.; Saito, M.; Oobatake, M.; Kanaya, S. *Biochemistry* **1995**, *34*, 6587−6601.
(9) Nicholson, L. K.; Kay, L. E.; Torchia, D. A. In *NMR Spectroscopy and Its Application to Biomedical Research*; Sarkar, S. K., Ed.; Elsevier: New York, 1996; pp 241−279.
(10) Zhu, L.; Prendergast, F. G.; Kemple, M. D. *J. Biomol. NMR* **1998**, *12*, 135−144.
(11) Coles, M.; Diercks, T.; Muehlenweg, B.; Bartsch, S.; Zolzer, V.; Tschesche, H.; Kessler, H. *J. Mol. Biol.* **1999**, *289*, 139−157.
(12) Guenneugues, M.; Gilquin, B.; Wolff, N.; Menez, A.; Zinn-Justin, S. *J. Biomol. NMR* **1999**, *14*, 47−66.
(13) Levy, R. M.; Karplus, M.; Wolynes, P. G. *J. Am. Chem. Soc.* **1981**, *103*, 5998−6011.
(14) Chandrasekhar, I.; Clore, G. M.; Szabo, A.; Gronenborn, A. M.; Brooks, B. R. *J. Mol. Biol.* **1992**, *226*, 239−250.
(15) Palmer, A. G., III.; Case, D. A. *J. Am. Chem. Soc.* **1992**, *114*, 9059−9067.
(16) Balasubramanian, S.; Nirmala, R.; Beveridge, D. L.; Bolton, P. H. *J. Magn. Res., Ser. B* **1994**, *104*, 240−249.
(17) Philippopoulos, M.; Lim, C. *J. Mol. Biol.* **1995**, *254*, 771−792.
(18) Smith, L. J.; Mark, A. E.; Dobson, C. M.; van Gunsteren, W. F. *Biochem.* **1995**, *34*, 10918−10931.
(19) Akke, M.; Bruschweiler, R.; Palmer, A. *J. Am. Chem. Soc.* **1993**, *115*, 9832−9833.
(20) Yang, D. Y.; Kay, L. E. *J. Mol. Biol.* **1996**, *263*, 369−382.
(21) Li, Z.; Raychaudhuri, S.; Wand, A. J. *Protein Sci.* **1996**, *5*, 2647−2650.
(22) Yang, D. Y.; Mok, Y.-K.; Forman-Kay, J. D.; Farrow, N. A.; Kay, L. E. *J. Mol. Biol.* **1997**, *272*, 790−804.
(23) Palmer, A. G., III.; Hochstrasser, R. A.; Millar, D. P.; Rance, M.; Wright, P. E. *J. Am. Chem. Soc.* **1993**, *115*, 6333−6345.
(24) Nicholson, L. K.; Kay, L. E.; Baldisseri, D. M.; Arango, J.; Young, P.; Bax, A.; Torchia, D. A. *Biochemistry* **1992**, *31*, 5253−5263.
(25) Engelke, J.; Ruterjans, H. *J. Biomol. NMR* **1998**, *11*, 165−183.
(26) Chatfield, D. C.; Szabo, A.; Brooks, B. R. *J. Am. Chem. Soc.* **1998**, *120*, 5301−5311.
(27) Brüschweiler, R.; Roux, B.; Blackledge, M.; Griesinger, C.; Karplus, M.; Ernst, R. R. *J. Am. Chem. Soc.* **1992**, *114*, 2289−2302.
(28) Blackedge, M. J.; Brüschweiler, R.; Griesinger, C.; Schmidt, J. M.; Xu, P.; Ernst, R. R. *Biochemistry* **1993**, *32*, 10960−10974.
(29) Brunne, R. M.; Gunsteren, W. F. v.; Brüschweiler, R.; Ernst, R. R. *J. Am. Chem. Soc.* **1993**, *115*, 4764−4768.
(30) Schmidt, J. M.; Brüschweiler, R.; Ernst, R. R.; Dunbrack, R. L. J.; Joseph, D.; Karplus, M. *J. Am. Chem. Soc.* **1993**, *115*, 8747−8756.
(31) Bremi, T.; Ernst, M.; Ernst, R. R. *J. Phys. Chem.* **1994**, *98*, 9322−9334.
(32) Bremi, T.; Brüschweiler, R.; Ernst, R. R. *J. Am. Chem. Soc.* **1997**, *119*, 4272−4294.
(33) Batchelder, L.; Niu, C. H.; Torchia, D. A. *J. Am. Chem. Soc.* **1983**, *105*, 2228−2231.
(34) Keniry, M. A.; Kintanar, A.; Smith, R. L.; Gutowsky, H. S.; Oldfield, E. *Biochemistry* **1984**, *23*, 288−298.
(35) Andrew, E. R.; Hinshaw, W. S.; Hutchins, M. G.; Sjoblom, R. O. I. *Mol. Phys.* **1976**, *5*, 1479−88.
(36) Andrew, E. R.; Hinshaw, W. S.; Hutchins, M. G.; Sjoblom, R. O. I.; Canepa, P. C. *Mol. Phys.* **1976**, *32*, 795−806.
(37) Andrew, E. R.; Hinshaw, W. S.; Hutchins, M. G.; Sjoblom, R. O. I. *Mol. Phys.* **1977**, *34*, 1695−1706.
(38) Gall, C. M.; DiVerdi, J. A.; Opella, S. J. *J. Am. Chem. Soc.* **1981**, *103*, 5039−5043.
(39) Beshah, K.; Griffin, R. G. *J. Magn. Res.* **1989**, *84*, 268−274.
(40) Lehmann, M. S.; Koetzle, T. F.; Hamilton, W. C. *J. Am. Chem. Soc.* **1972**, *94*, 2657−2660.
(41) Brooks, B. R.; Bruccoleri, R. E.; Olafson, B. D.; States, D. J.; Swaminathan, S.; Karplus, M. *J. Comput. Chem.* **1983**, *4*(2), 187−217.
(42) Mackerell, A. D., Jr.; Bashford, D.; Bellot, M.; Dunbrack, R. L.; Field, M. J.; Fischer, S.; Gao, J.; Guo, H.; Joseph, D.; Ha, S.; Kuchnir, L.; Kuczera, K.; Lau, F. T. K.; Mattos, C.; Michnick, S.; Nguyen, D. T.; Ngo, T.; Prodhom, B.; Roux, B.; Schlenkrich, B.; Smith, J.; Stote, R.; Straub, J.; Wiorkiewicz-Kuczera, J.; Karplus, M. *J. Phys. Chem. B* **1998**, *102*, 3586−3616.
(43) Essmann, U.; Perera, L.; Berkowitz, M. L.; Darden, T.; Lee, H.; Pedersen, L. G. *J. Chem. Phys.* **1995**, *103*, 8577−8593.
(44) Darden, T.; York, D.; Pedersen, L. G. *J. Chem. Phys.* **1993**, *98*, 10089−10092.
(45) Steinbach, P. J.; Brooks, B. R. *J. Comput. Chem.* **1994**, *15*, 667.
(46) Frisch, M. J.; Trucks, G. W.; Head-Gordon, M.; Gill, P. M. W.; Wong, M. W.; Foresman, J. B.; Johnson, B. G.; Schlegel, H. B.; Robb, M. A.; Replogle, E. S.; Gomperts, R.; Andres, J. L.; Raghavachari, K.; Binkley, J. S.; Gonzalez, C.; Martin, R. L.; Fox, D. J.; Defrees, D. J.; Baker, J.; Stewart, J. J. P.; Pople, J. A. *Gaussian 92, Revision A;* Gaussian, Inc.: Pittsburgh, PA, 1992.
(47) Lipari, G.; Szabo, A. *J. Am. Chem. Soc.* **1982**, *104*, 4546−4559.
(48) Press: W. H.; Teukolsky, S. A.; Vetterling, W. T.; Flannery, B. P. *Numerical Recipes in Fortran*; Cambridge University Press: New York, 1992; pp 678−683.
(49) Zwanzig, R.; Ailawasi, N. *Phys. Rev.* **1969**, *182*, 280.
(50) Loncharich, R. J.; Brooks, B. R.; Pastor, R. W. *Biopolymers* **1992**, *32*, 523−535.
(51) Medhi, J. *Stochastic Processes*; Wiley: New York, 1982.
(52) Crow, E. L.; Gardner, R. S. *Biometrika* **1959**, *46*, 441−453.
(53) Pastor, R. W.; Feller, S. E. In *Biological Membranes, A Molecular Perspective from Computation and Experiment*; Merz, K. M., Roux, B., Eds.; Birkhäuser: Boston, 1996; pp 4−29.
(54) Brunger, A.; Brooks, C. L.; Karplus, M. *Chem. Phys. Lett.* **1984**, *105*, 495.
(55) Pastor, R. W.; Brooks, B. R.; Szabo, A. *Mol. Phys.* **1988**, *65*, 1409.
(56) Gunsteren, W. F. v.; Berendsen, H. J. C. *Mol. Phys.* **1982**, *45*, 637.
(57) Eyring, H. *Quantum Chemistry*; Wiley: New York, 1944; p 310.
(58) Stejskal, E. O.; Gutowsky, H. S. *J. Chem. Phys.* **1958**, *28*, 388−396.
(59) Shirts, R. B. *ACM Trans. Math. Software* **1993**, *19*, 377−390.
(60) Shirts, R. B. *ACM Trans. Math. Software* **1993**, *19*, 391−406.
(61) Torchia, D. A.; Szabo, A. *J. Magn. Res.* **1982**, *49*, 107−121.
(62) Edholm, O.; Blomberg, C. *Chem. Phys.* **1979**, *42*, 449−464.